Mon. Not. R. astr. Soc. (1989) **239**, 1–17

The giant haloes of NGC 6543 and 6826

D. Middlemass and R. E. S. Clegg* *Department of Physics and Astronomy, University College London, Gower Street, London WC1E 6BT*

J. R. Walsh† *Kapteyn Astronomical Institute, 9700 AV Groningen, The Netherlands*

Accepted 1988 October 20. Received 1988 September 8

Summary. Long-slit spectra at several positions on the large, faint haloes of NGC 6543 and 6826, from IPCS and CCD detectors, are analysed to give average properties of these two regions. Comparison of the halo and bright core spectra shows that the halo emission is thermal and not reflection. Average halo properties and masses are estimated. The [O III] electron temperature is higher in each halo than in its central nebula; we find T_e (halo) = 14 700 and 13 000 K for NGC 6543 and 6826, respectively. The mass ratios (halo/core) are in the range 2.9–10.2 and 0.07–2.24 for NGC 6543 and 6826, respectively, from absolute Hβ flux measurements at representative slit positions. Both haloes appear to have lower abundances than their bright cores.

Photo-ionization models are used with limited success to reproduce the conditions of the haloes. 'Pre-hardening' of the ionizing radiation field by optically thick inner cores does not produce sufficient heating to explain the observed high T_e values. It is suggested that the hot fast stellar wind in NG 6543 has escaped beyond the central nebula and has shocked the filamentary halo.

1 Introduction

NGC 6543 and 6826 are members of a group of planetary nebulae (PNe) now known as multiple shell planetary nebulae, a phase through which more than half of PNe are observed to pass during their lifetime (Chu, Jacoby & Arendt 1987). In particular these two objects are classified as Type I multiple shell PNe or 'faint halo PNe' due to their large outer shells which are on average about 10^3 to 10^4 times less bright than the main core of the nebula.

These outer haloes are of great interest as they are presumably the remains of the original stages of mass loss from the progenitor stars. In studying them we probe the state of the outer layers of the progenitor, perhaps before all of the mixing of elements from the core to the outer envelope has been completed. The mass of a halo forms part of the difference between the mass of the central star as observed now and its progenitor. This difference must be measured so as to calibrate the initial mass–final mass relation for stellar evolution. Theory predicts that AGB stars with initial masses of, for example, 1 and 2 $M_\odot$ can evolve to central stars of 0.55 and 0.62 $M_\odot$ respectively (e.g. Kwok 1983). The mass lost (0.45–1.38 $M_\odot$) should be present in the form of a PN or neutral shell around the central star.

*Present address: Royal Greenwich Observatory, Herstmonceux Castle, Hailsham, East Sussex BN27 1RP.
†Present address: ST ECF, ESO, Karl-Schwarzschild-Strasse 2, D-8046 Garching bei Munchen, FRG.

Capriotti (1978) discussed the origins of PNe giant haloes, and showed that they could contain very large masses of gas. Assuming that the sharp edges of NGC 6543 and 6826 represented the Strömgren radii for the central stars, he gave halo masses of 24 and 8 $M_\odot$, respectively for these systems, for adopted electron densities of 130 and 360 cm^{-3}. If correct, these masses would be extremely important for comparison of PNe with stellar evolution theory.

The observations presented here were undertaken to measure the properties, including the temperature, density and mass of the haloes, Hippelin, Baessgen & Grewing (1985) observed the two multiple shell PNe studied here and NGC 7662: they used annular diaphragms which occulted the core of the PN but had to make large corrections for light scattered by the observing system from the core. We have used long slit spectroscopic observations offset from the core to study these objects more fully.

2 Observations

The data were obtained with the 2.5-m Isaac Newton Telescope at La Palma on 1987 July 22–24 under seeing conditions of about 1.5 arcsec, and grey to dark Moon. We employed the Intermediate Dispersion Spectrograph with an IPCS detector (format 126 × 2048 pixels) on the 235-mm camera and a GEC CCD on the 500-mm camera. With the IPCS setup we used different gratings to provide low-dispersion spectra in the range 3600–7600 Å and high-dispersion spectra in the range 3600–4600 Å. The resolutions of these are 4.0 and 1.0 Å, respectively. With the CCD, spectra from 5400–7600 Å with a resolution of 2.7 Å were taken.

For exposures of the bright cores we made use of neutral density filters whose spectral transmission responses were corrected for in the image processing. Slit widths were of the order of 0.8 arcsec for the PN cores and 1.6–3 arcsec for the haloes. All standard stars were observed with slit widths of 5.4 arcsec. Great care was taken with the IPCS images to ensure that emission lines with pixels of count rates higher than 0.5 Hz were not used, as these may have saturated due to the slowness of the event centering software with such a large format.

The 2-dimensional images were processed using the FIGARO software, written by Keith Shortridge (see Bridger 1987), on the UCL node of the SERC STARLINK network. The images for each night were corrected for atmospheric extinction using photometric measurements made by the Carlsberg Automatic Meridian Circle. Flux calibration was achieved with wide-slit observations of a number of standard stars from Stone (1977) and Oke (1974).

We observed a number of positions in the nebular haloes in order to determine their 'average' properties. The slit positions are indicated in Plates 1 and 2. These are both based on the plates of Millikan (1974) and are broad-band images taken on IIIa-J emulsion and thus probably dominated by [O III]$\lambda\lambda$5007, 4959 and Hβ. The NGC 6543 plate has been processed by D. F. Malin to enhance the contrast. We also observed the bright inner core of each PN with the slit offset from the centre of the nebula to avoid the bright central star. The positions were 3 arcsec north-east, position angle 140° for NGC 6543 and 5 arcsec east, position angle 124° for NGC 6826. For each slit position there were usually two images exposed with integration times of about 1800 s each. After processing, the two images were added to increase the signal-to-noise ratio.

The images were examined for emission in lines such as Hα, [O III]λ5007 and [O II]λ3727 and a spectrum extracted in the regions where such emission was found. The locations of the edges of the halo in our images coincided well with those seen on Plates 1 and 2. The angular radii of the NGC 6543 and 6826 haloes are 165 and 72 arcsec, and for our adopted distances (see Section 3) these correspond to linear radii of 0.89 and 0.80 pc. In all slit positions the slit protruded from the halo into the sky and the pixels there were used for sky subtraction. An

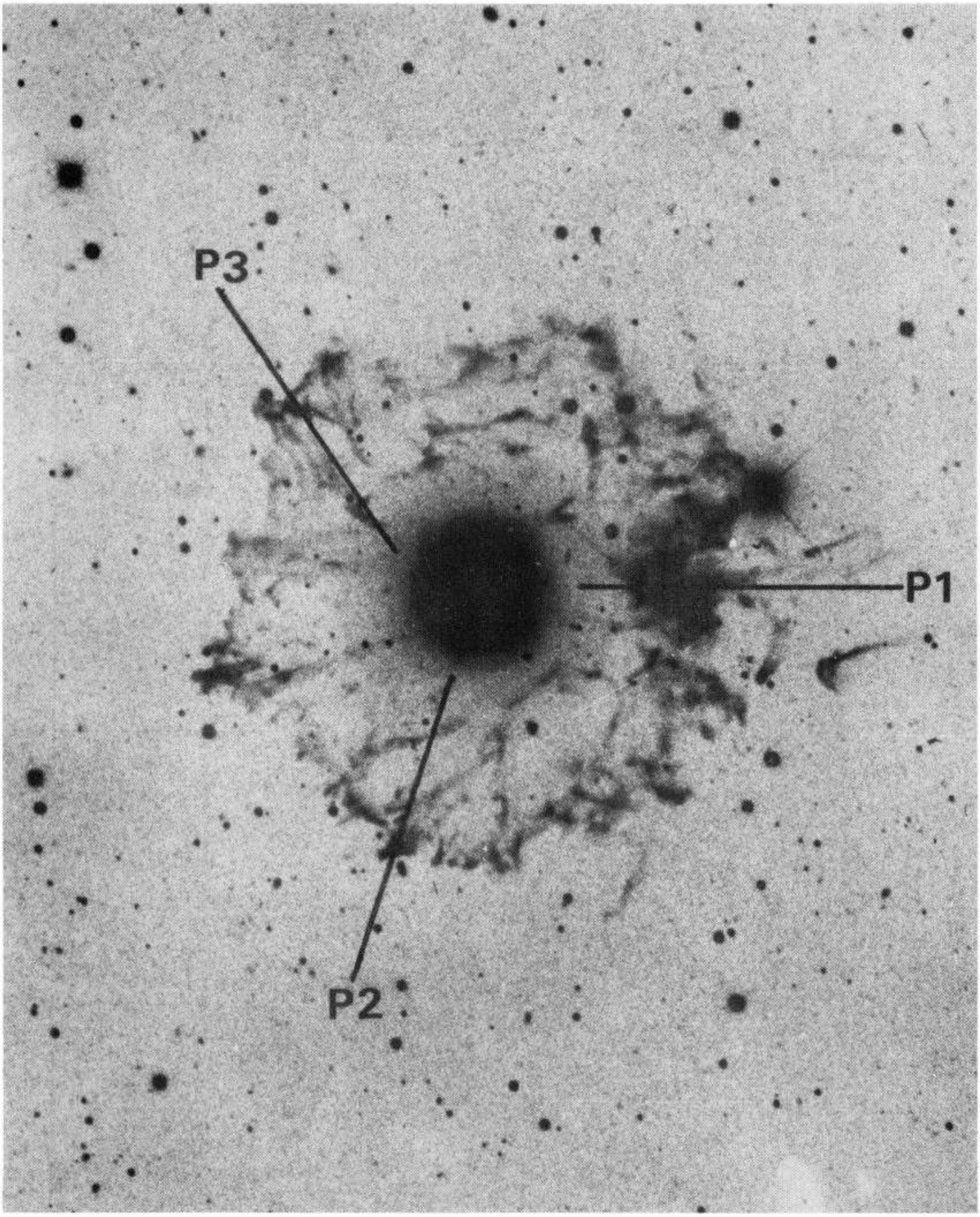

Plate 1. Deep exposure of the planetary nebula NGC 6543 showing details of the giant halo, with the inner nebula highly overexposed. North is at the top with east to the left. The slit positions marked are those at which we made observations. Note the filaments in the south-west outside the halo which are probably density enhancements in a large outer shell. This plate (by Millikan) has been contrast-enhanced by D. F. Malin.

[*facing page* 2]

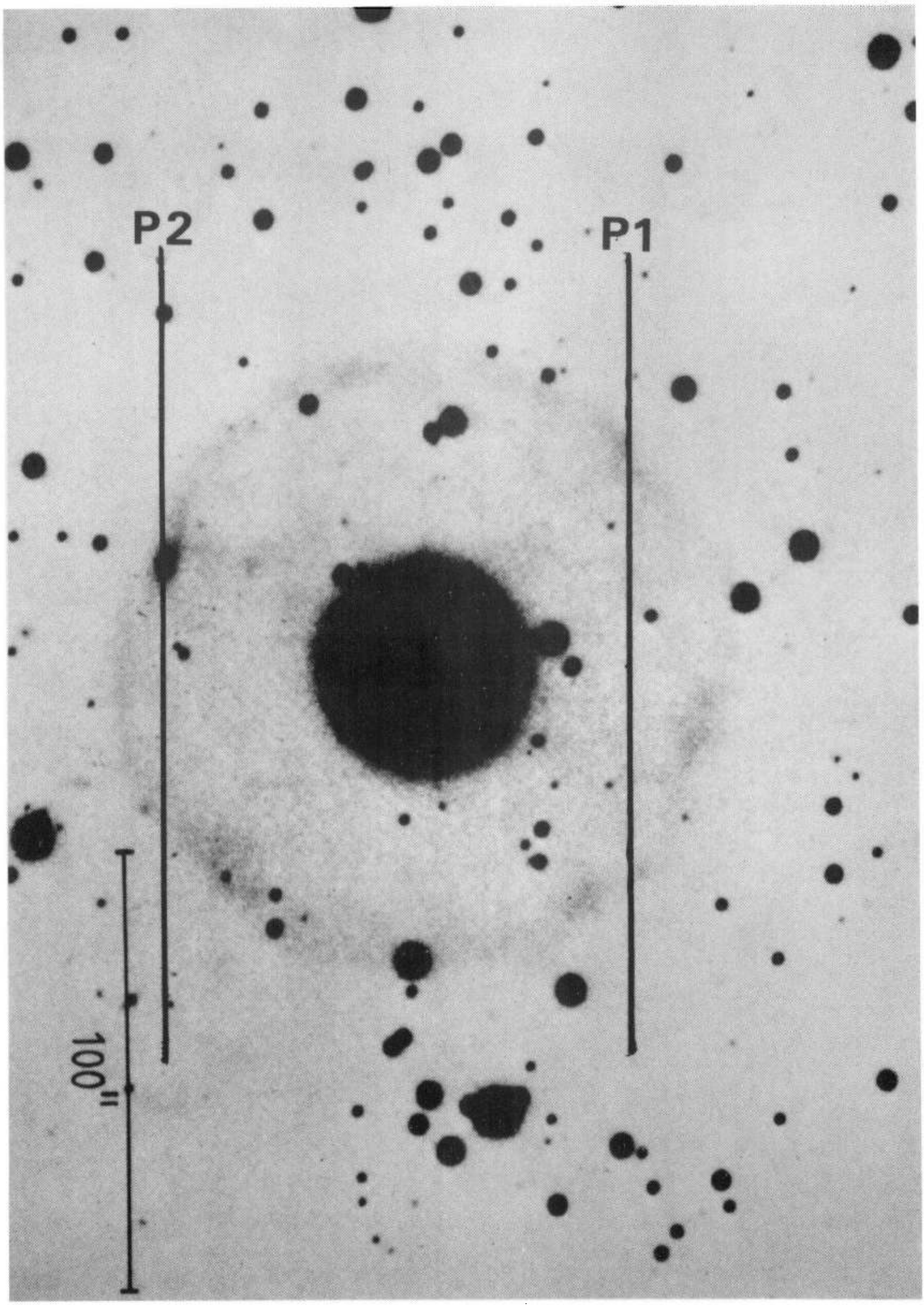

Plate 2. Deep exposure of the planetary nebula NGC 6826 showing its halo. The slit positions marked are those at which we made observations. The emission in the knot at the north edge of the halo on slit position 2 was found to be thermal.

example of this is given in Fig. 1, part of a 1.0 Å resolution spectrum of the halo of NGC 6543 at slit position 1. Panel (a) shows the gross spectrum of the halo, (b) the sky background in an equivalent number of spatial pixels and (c) the net PN spectrum after sky subtraction. Note the absence of Hγ emission in the sky, in which only Hg I λ4358.33 is observed and is accurately subtracted from the PN spectrum.

In Figs 2–4 we present results for the variation of ionic line emission with position along the slit. Fig. 2 indicates that the [O III]5007 Å emission across NGC 6826 is quite patchy. If Plate 2 were reprocessed with contrast enhancement (as has been done in Plate 1 for NGC 6543) this halo might well appear filamentary also. The CCD frame presented by Jewitt *et al.* (1986) shows signs of filamentary structure in the halo. Figs 3 and 4 show the rise in the O^+/O^{2+} ratio in filaments and at the very edge of the NGC 6543 halo. The effects of differential atmospheric refraction are not significant for these diagrams. This spatial information is discussed further in Section 4.

For NGC 6543 we also used low-resolution large aperture *IUE* data. These were obtained from the World Data Center at the Rutherford Appleton Laboratory and the data were extracted using the STARLINK IUEDR software (Giddings 1983). The image SWP 20122 of the bright western knot in the halo (see Plate 1) provided a measurement of C III]λ1908. For

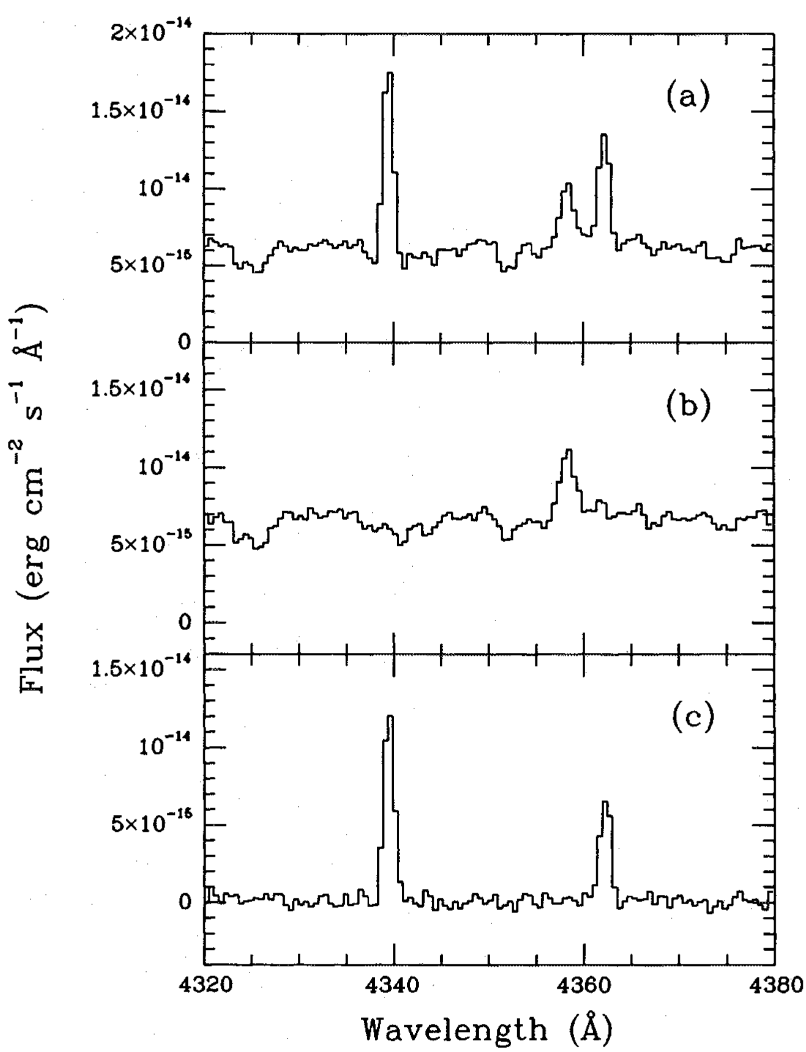

Figure 1. Spectra of the west knot of NGC 6543 taken with a 1200 l mm^{-1} grating: (a) gross spectrum, (b) local sky spectrum in equivalent number of pixels and (c) sky subtracted spectrum. Note the accurate sky subtraction (including the Hg line at 4358 Å) and the large strength of [O III] 4363 Å.

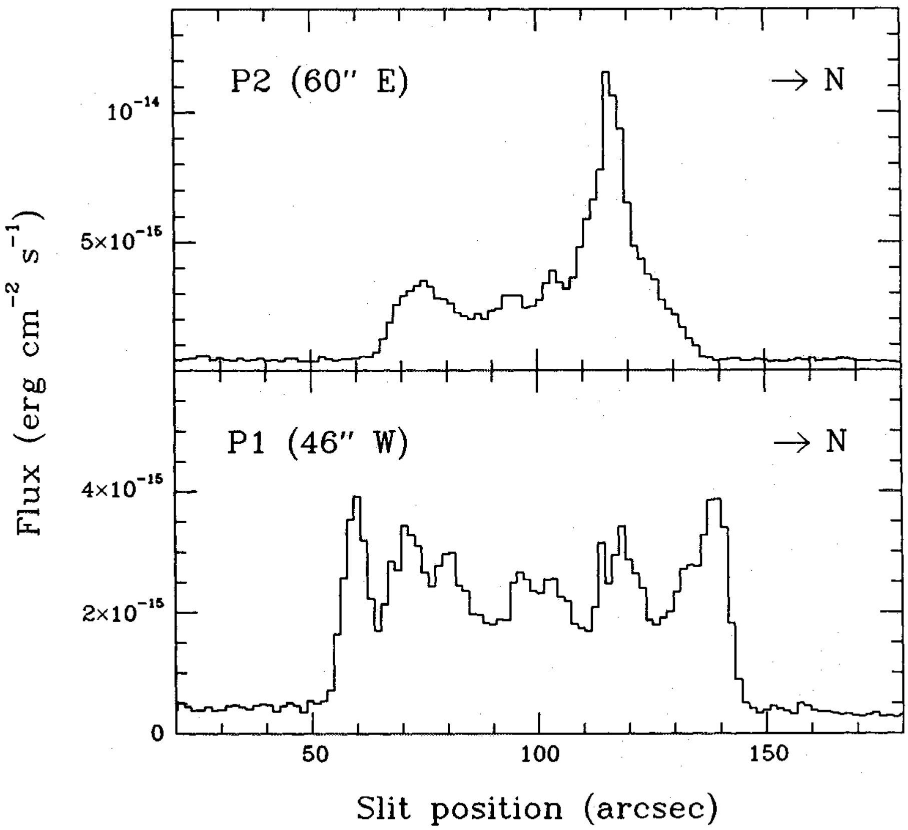

Figure 2. Spatial variation along the slit in the emission line [O III]λ5007 for NGC 6826. Each slit position was oriented N–S and offset by the distance given in the plots (see Plate 2).

comparison with this we have also used the images SWP 1897, LWR 1761 and LWR 2925 of the core of the PN. These have detectable emission in C IV, C III] and [C II]. However, the C IV line originates in the stellar wind and is not representative of the nebula itself. We believe the other carbon lines to be of nebular origin as they are not present in the small aperture image of SWP 1897, as shown by Castor, Lutz & Seaton (1981), which was centred on the central star. The emission line fluxes of the core were corrected – for the limited size of the large aperture relative to the size of the PN core – by multiplying by 4.0. This value is the ratio of the effective area of the Hα isophote map of Phillips, Reay & Worswick (1977) to the area of the large aperture. The halo C III] emission line flux was calibrated via our measurement of the Hβ emission per arcsec^2 in the west knot.

It is important to assess any contribution to the measured halo fluxes due to telescopic scattering. To estimate this for the *IUE* image of the west knot, we used the empirical formula for the SWP large aperture given by Witt *et al.* (1982). From this we find the contribution due to instrumental scattering of the light from the core, at an offset of 100 arcsec, to be less than 1 per cent of the observed flux. The west knot is 120 arcsec from the central star and about 75 arcsec from the edge of the nebula. Tests carried out on the INT with a slit offset 12 arcsec from a bright star and orientated tangentially showed no detection greater than that which would be expected from the far-field seeing disc of the star (King 1971). At the (greater) offsets used here to observe the haloes, the scattering contribution, from telescope and sky effects, is not significant.

We have combined the results from the different slit positions to produce average fluxes for each halo. (The surface brightness is too low to permit abundance analyses of radial filaments.)

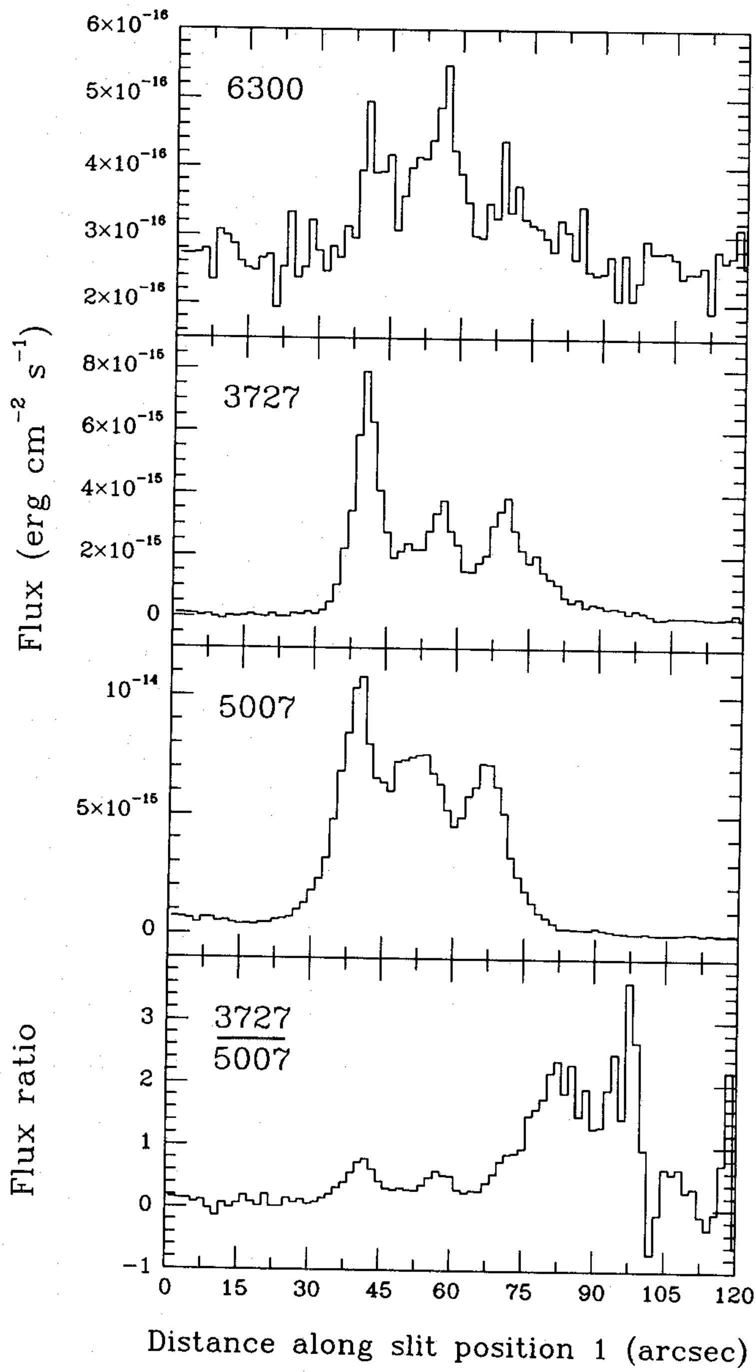

Figure 3. Spatial variation, along slit position 1 of [O I]λ6300, [O II]λ3727, [O III]λ5007, and the ratio of 3727/5007 in NGC 6543. The nebular centre would be at −55 arcsec in this figure.

The average fluxes (corrected for interstellar extinction) are presented in Tables 1 and 2. Values for the extinction constant, *c*, for each nebula were found from our measurements of the Balmer Decrement, and are in agreement with values given by Kaler (1976). The [Ne III] 3868 Å line in the NGC 6543 core was either saturated or contaminated by noise in our spectra and we used the measurement of Aller & Czyzak (1979) for this line. The errors are estimated at 10 per cent for strong lines and 30 per cent for weak lines, from photon noise and uncertainty in placement of the continuum level.

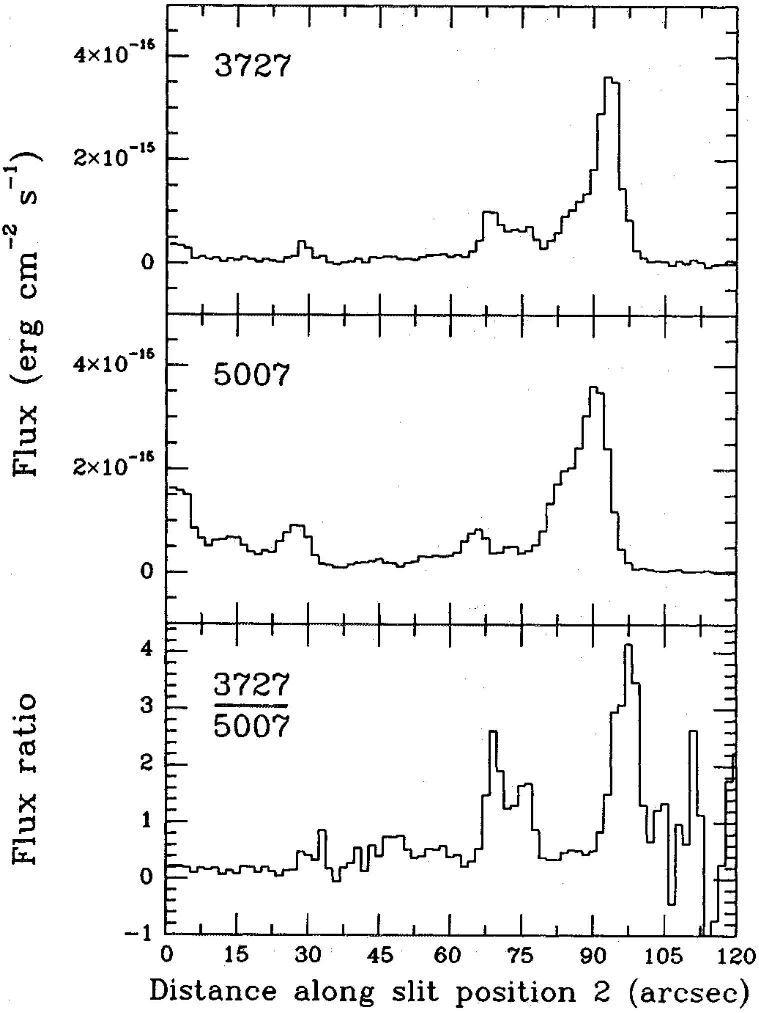

Figure 4. Spatial variation, alon slit position 2 of [O II]λ3727, [O III]λ5007, and their ratio in NGC 6543. The sharp rise in the ratio at the edge of the halo is real and is not due to misregistration of the spectra or atmospheric dispersion effects. The nebular centre would be at −51 arcsec in this figure.

3 Results

3.1. ELECTRON DENSITY AND TEMPERATURE

We used the lines of oxygen to determine electron temperatures and densities, with T_e measured from [O III]λλ4959+5007/4363, and N_e from [O II]λλ3729/3726. In Table 3 we give the line ratios measured in both the core and halo of each object and the results which these imply.

Unfortunately the diagnostic ratio for N_e is at, or for NGC 6826 is consistent with, the low density limit: the error bars on the λλ3729/3726 ratio always include the low density value of 1.50. We can only give an upper limit to the electron density with any certainty although we can explore the consequences of the nominal measured density for NGC 6826. Of great interest is the difference found between T_e values of the core and halo in both PNe. The high T_e measurement in the halo is due to the relatively large strength of [O III]λ4358. We checked that this is not due to an incorrect sky subtraction, with some remaining Hg I λ4360 emission perhaps corrupting the [O III] measurement. Fig. 1 (for NGC 6543) illustrates that these two lines were

Table 1. Average, dereddened ($c = 0.2$) line fluxes for NGC 6543.

λ (Å)	Identity	f(λ)	Core I(λ)	Halo I(λ)
1908	C III]	1.285	30.8	852.0
2326	[C II]	1.413	6.5	—
3727	[O II]	0.256	23.9	1010.0
3868	[Ne III]	0.230	(60.3)	132.1
3967	"	0.210	—	64.2
4101	Hδ	0.182	28.0	27.7
4267	C II	0.144	0.5	—
4340	Hγ	0.127	44.8	47.5
4363	[O III]	0.121	1.8	28.1
4388	He I	0.116	0.9	—
4471	He I	0.095	5.3	—
4712	[Ar IV]	0.037	1.6	—
4861	Hβ	0.000	100.0	100.0
4922	He I	-0.015	1.7	—
4959	[O III]	-0.024	227.3	518.0
5007	"	-0.036	663.0	1528.0
5876	He I	-0.215	15.6	8.4
6300	[O I]	-0.282	0.9	27.5
6547	[N II]	-0.318	5.7	96.1
6583	"	-0.323	16.8	291.2

Note: The value in parenthesis is from Aller & Czyzak (1979).

resolved and a good sky subtraction obtained. The strength of $\lambda 4363$ relative to Hγ can be clearly seen in the figure.

3.2 ABUNDANCES

Elemental abundances for the PN cores and the haloes have been derived using the same consistent methods where possible. Comparisons of the compositions of different shells of multiple shell PNe are of great interest, as the regions may represent ejection events occurring at different times ($\Delta t \sim 10^5$ yr) during the evolution of the progenitor red giant star.

The adopted fluxes listed in Tables 1 and 2 have been used to obtain empirical abundances for the adopted N_e and T_e values in Table 3. The atomic data used are from the compilation of Mendoza (1983) except for more recent collision strengths for Ne III (Butler & Mendoza 1984). Ionization correction factors (icfs) were taken from Barker (1983) except for carbon; the carbon icfs for the NGC 6543 core and halo are from the PN photo-ionization model described in Section 3.4.1. This was adopted because the average level of ionization in this halo is similar to that of the core; the halo icf is probably then uncertain to a factor 2, but the

Table 2. Average, dereddened ($c = 0.04$) line fluxes for NGC 6826.

λ (Å)	Identity	f(λ)	Core I(λ)	Halo I(λ)
3727	[O II]	0.256	20.9	81.7
3868	[Ne III]	0.230	48.3	69.2
3967	"	0.210	15.4	16.1
4101	Hδ	0.182	28.5	28.7
4267	C II	0.144	0.9	—
4340	Hγ	0.127	47.0	48.0
4363	[O III]	0.121	5.5	11.3
4471	He I	0.095	5.1	—
4712	[Ar IV]	0.037	1.2	—
4861	Hβ	0.000	100.0	100.0
4922	He I	-0.015	1.5	—
4959	[O III]	-0.024	253.0	274.0
5007	"	-0.036	770.0	797.0
5876	He I	-0.215	14.9	7.3
6300	[O I]	-0.282	—	2.6
6547	[N II]	-0.318	3.1	—
6583	"	-0.323	8.2	8.3

Table 3. T_c and N_c from measured emission line ratios.

	NGC 6543		NGC 6826	
	core	halo	core	halo
I(4959+5007)/I(4363)	492 ± 88	72.8 ± 9.0	184.5 ± 37	94.8 ± 47
T_e (K)	7900^{+400}_{-300}	14700^{+900}_{-800}	10400^{+750}_{-600}	13000^{+5000}_{-1700}
I(3729)/I(3726)	0.47 ± 0.05	1.44 ± 0.12	0.65 ± 0.07	1.07 ± 0.5
N_e (cm^{-3})	5140^{+3900}_{-1600}	35^{+100}_{-35}	2000^{+700}_{-550}	450^{+2700}_{-450}

resulting uncertainty due to this in N(C)/N(H^+) is only 20 per cent. The elemental abundances in Tables 4 and 5 are calculated assuming negligible fractions of neutral H and He in the haloes. The effect of such neutral gas is discussed in Section 3.4.2.

The icfs used were compared with the predictions of the photo-ionization models. The model correction factor for neon is in very good agreement with the empirical icf of Barker (1983), but the correction factors for nitrogen, icf (N^+), are both a factor 1.25 higher than Barker's. This does not affect our comparison of halo and core abundances, but it should be noted that the N abundance values given may be only 80 per cent of the actual abundances.

Table 4. Empirical abundances* for NGC 6543.

		Core	Halo	$\frac{N(X)_{halo}}{N(X)_{core}}$
O	O^{2+}	58.4^{+12}_{-9}	$17.9^{+2.0}_{-1.5}$	
	O^{+}	$5.11^{+3.9}_{-1.5}$	$9.05^{+3.9}_{-2.8}$	
	O^{o}	$0.47^{+0.09}_{-0.09}$	$1.57^{+0.6}_{-0.6}$	
	icf	1.0	1.0	
	N(O)/N(H)	$64.0^{+16}_{-10.6}$	$28.5^{+6.5}_{-5.0}$	$0.45^{+0.15}_{-0.11}$
	AC 1983	56.0		
Ne	Ne^{2+}	$14.6^{+3.2}_{-3.2}$	$3.31^{+0.9}_{-0.6}$	
	icf	$1.10^{+0.04}_{-0.02}$	$1.59^{+0.17}_{-0.16}$	
	N(Ne)/N(H)	$16.0^{+4.0}_{-3.7}$	$5.27^{+2.14}_{-1.40}$	$0.33^{+0.16}_{-0.11}$
	AC 1983	14.1		
N	N^{+}	$0.67^{+0.13}_{-0.11}$	$2.28^{+0.5}_{-0.4}$	
	icf	$12.5^{+2.3}_{-3.6}$	$3.15^{+0.61}_{-0.45}$	
	N(N)/N(H)	$8.38^{+0.02}_{-1.26}$	$7.18^{+0.33}_{-0.11}$	$0.85^{+0.04}_{-0.13}$
	AC 1983	8.71		
C	C^{2+}	61.5^{+29}_{-23}	22.8^{+6}_{-4}	
	C^{+}	$5.66^{+2.1}_{-1.8}$	—	
	icf	1.13	1.25	
	N(C)/N(H)	75.7^{+35}_{-28}	$28.5^{+7.5}_{-5}$	$0.38^{+0.20}_{-0.16}$
He	N(He)/N(H)	$0.11^{+0.01}_{-0.01}$	$0.06^{+0.02}_{-0.02}$	$0.55^{+0.21}_{-0.21}$

*Given as $10^5\,(X^i/H^+)$ except for helium.

The core abundances for NGC 6543 are only 10 per cent different, on average, from the results of Aller & Czyzak (1983, AC). The core abundances of NGC 6826 are, however, significantly different from those of Barker (1988), the largest discrepancy being for neon. Barker states that Aller & Czyzak now quote 4×10^{-5} for the neon abundance, their 1983 published value being in error. Their new value agrees well with ours. The higher value of Barker may be due partly to his lower adopted electron temperature, and partly to use of different atomic data. For Ne III we use the recent collision strengths of Butler & Mendoza (1984).

Table 5. Empirical abundances* for NGC 6826.

		Core	Halo	$\frac{N(X)_{halo}}{N(X)_{core}}$
O	O^{2+}	$23.8^{+5.4}_{-4.8}$	11.1^{+7}_{-3}	
	O^{+}	$0.88^{+0.35}_{-0.20}$	$1.70^{+1.3}_{-0.6}$	
	O^{o}	—	$0.19^{+0.1}_{-0.05}$	
	icf	1.0	1.0	
	N(O)/N(H)	$24.7^{+5.8}_{-5.0}$	$13.0^{+8.3}_{-3.6}$	$0.53^{+0.36}_{-0.18}$
	Barker 1988	40		
Ne	Ne^{2+}	$3.47^{+0.95}_{-0.72}$	$1.64^{+0.8}_{-0.5}$	
	icf	$1.04^{+0.005}_{-0.003}$	$1.17^{+0.007}_{-0.010}$	
	N(Ne)/N(H)	$3.61^{+1.0}_{-0.8}$	$1.92^{+0.95}_{-0.60}$	$0.53^{+0.30}_{-0.20}$
	Barker 1988	9.2		
N	N^{+}	$0.15^{+0.03}_{-0.02}$	$0.15^{+0.05}_{-0.03}$	
	icf	$28.07^{+0.90}_{-3.27}$	$7.65^{+0.90}_{-0.55}$	
	N(N)/N(H)	$4.21^{+0.25}_{-0.44}$	$1.15^{+0.27}_{-0.12}$	$0.27^{+0.07}_{-0.04}$
	Barker 1988	5.1		
He	N(He)/N(H)	$0.10^{+0.01}_{-0.01}$	$0.05^{+0.02}_{-0.02}$	$0.50^{+0.20}_{-0.20}$

*Given as $10^5\,(X^{i}/H^{+})$ except for helium.

3.3. HALO MASSES

We calculated the mass of ionized gas in the haloes from the absolute Hβ flux and the limits on the electron density (see below). Our measurements of Hγ and Hβ yielded average absolute Hβ fluxes per arcsec^2 for each halo, after careful inspection of the spectra and of Plates 1 and 2. Table 7 gives these mean values, together with our adopted values of the projected area of the halo, absolute Hβ fluxes for the cores, nebular distances and resulting masses. The core Hβ fluxes are taken from Kaler (1983, 1978) for NGC 6543 and 6826, respectively. The distances used were those given by Cudworth (1974).

We found that the large, bright knot west of NGC 6543 is brighter than the rest of the halo by a factor of about 6, and we used measurements from positions 2 and 3 in this object to represent the average Hβ surface brightness. Similarly, a small bright knot in the NGC 6826 halo was ignored for that halo.

Considering both haloes to be spheres of angular radius θ_H (with a core of radius θ_C), filled with material of electron density N_e at temperature $t_e = T_e/10^4$ K and a volume filling factor ε,

Table 6. Photoionization model results for PN cores.

	NGC 6543				NGC 6826			
	X^o	X^+	X^{2+}	X^{3+}	X^o	X^+	X^{2+}	X^{3+}
H	0.001	0.999			0.001	0.999		
He	0.003	0.997	0.000		0.002	0.998	0.000	
C	0.000	0.088	0.799	0.011	0.000	0.053	0.781	0.165
N	0.000	0.058	0.821	0.121	0.000	0.031	0.802	0.167
O	0.000	0.070	0.930	0.000	0.000	0.038	0.962	0.000
Ne	0.000	0.052	0.948	0.000	0.000	0.029	0.971	0.000
S	0.000	0.001	0.459	0.500	0.000	0.005	0.347	0.614

Adopted parameters:

Star T_{eff}	40 000 K	45 000 K
L	6600 $L_\odot$	10000 $L_\odot$
log g	4.0	4.0
He/H	0.10	0.10
Distance	1.1 kpc	2.3 kpc

Table 7. Ionized masses.

	NGC 6543	NGC 6826
$I(H\beta)_{halo}$ (erg/cm/s/arcsec^2)	5.40 x10^{-17}	1.12 x10^{-16}
Halo area (arcsec^2)	85500	16300
$I(H\beta)_{core}$ (erg/cm/s)	4.07 x10^{-10}	1.27 x10^{-10}
Distance (kpc)	1.1	2.3
Core mass ($M_\odot$)	$0.09^{+0.02}_{-0.04}$	$0.42^{+0.16}_{-0.11}$
N_e [1] (cm^{-3})	9.9±1.8	14.4±2.7
Halo mass ($M_\odot$)	$0.92^{+0.17}_{-0.92}$	$0.94^{+0.17}_{-0.94}$
N_e [2] (cm^{-3})	35^{+100}_{-35}	450^{+2700}_{-450}
Halo mass ($M_\odot$)	$0.26^{+\infty}_{-0.19}$	$0.03^{+\infty}_{-0.026}$

1. N_c calculated from equation (1) with $\varepsilon = 1$.
2. N_c calculated from [O II] doublet ratio.

we use the two formulae given by Clegg, Peimbert & Torres-Peimbert (1987) – adapting equation (1) to give the absolute dereddened Hβ flux of the halo – thus,

$$F(\mathrm{H}\beta)=1.45\times10^{-20}N_e^2\,\varepsilon(\theta_\mathrm{H}^3-\theta_\mathrm{C}^3)\,d\,t_e^{-0.88}/(1+y^+ +2y^{2+}) \quad (1)$$

and

$$M_i=8.07\times10^{11}F(\mathrm{H}\beta)\,d^2\,t_e^{0.88}(1+4y)/N_e \quad (2)$$

where d is the distance in kpc and y = N(He)/N(H), (y^+ and y^{2+} are the ionic abundances for singly and doubly ionized helium, respectively). By rearranging (1) and solving for $N_e^2\varepsilon$ we can put $\varepsilon=1$ and obtain lower limits to the electron density (this is the so-called rms electron density). The results are 9.85 ± 1.80 and 14.38 ± 2.70 cm^{-3} for NGC 6543 and 6826, respectively. Equation (2) was used with these lower limits to the electron density and the upper limits found from the [O II] $\lambda\lambda$3729/3726 line ratio, to give limits of the halo ionized masses (Table 7). We find the halo ionized masses to be in the range 0.26–0.92 $M_\odot$ for NGC 6543 and 0.03–0.94 $M_\odot$ for NGC 6826. (A possible neutral component is discussed in Section 4.) Note that if the haloes are hollow shells rather than filled spheres, the upper limits to the mass are reduced but the lower limits are unchanged. Also note that, while the limits on M_i(halo) depend on adopted distance, the ratio of halo mass to core mass is independent of distance.

3.4 ANALYSIS WITH PHOTO-IONIZATION MODELS

Photo-ionization models have been used to explore the nature of both PN cores and haloes. The code used is that described by Harrington *et al.* (1982). The code allows the use of multiple shells but not with different abundances, thus models with haloes were made to try and reproduce the physical characteristics of the haloes but not with the effects of abundance gradients. All of the models discussed here were fully converged and included transfer of the diffuse radiation field.

3.4.1 *The PN cores*

The core models were constructed with density structures obtained by measuring the Hα isophotes given by Phillips *et al.* (1977) for NGC 6543 and Phillips & Reay (1983) for NGC 6826. We decided to use non-LTE model atmospheres (Clegg & Middlemass 1987) as the best representation of a central star available to us. For NGC 6543 we tried using the stellar parameters given by Lucy & Perinotto (1987) who obtained T = 56 000 K. However, we found that this provided too much heating. The Zanstra temperature for this star is 43 000 K (Castor *et al.* 1981) and we obtained a good model match with a non-LTE model atmosphere with T = 40 000 K. Note that the existence of an ionized halo implies the core of the PN is not optically thick in all directions, but even if half of the photons escape, the effect on T_{Zan} is small. Our photo-ionization model matched the Hβ flux exactly, T_e and N_e diagnostic line ratios to within 8 per cent and other line fluxes to within 10 per cent – except [O I] λ6300 which was a factor 100 too small.

We adopted a temperature of 45 000 K and log g = 4 for the central ionizing source of NGC 6826. The stellar luminosity was 10 000 $L_\odot$. This model matched the Hβ flux exactly, and T_e and N_e diagnostic line ratios and other line fluxes to within 12 per cent. Results from these models are presented in Table 6 together with the adopted parameters.

3.4.2 The PN haloes

In order to test whether the high halo electron temperatures observed could be produced by photoelectric heating, uniform haloes, with the densities given in Table 3, were added to the core models for both PNe. For each computed model the filling factor of the halo was adjusted until the correct halo Hβ flux was produced. For the models with the original core parameters, the halo temperature was fairly constant with radius but at a slightly lower value than for the core, for both PNe. To increase the halo T_e the central star luminosity was decreased to make the model more optically thick and so 'harden' the radiation field illuminating the haloes. We found that this served to increase T_e(halo) until τ(H I), the optical depth in the Lyman continuum, reached about 30 when the halo temperature started to drop rapidly (as the hydrogen becomes neutral.)

Figure 5 shows diagrams of T_e versus radius for various models labelled with τ(H I), the curve with the lowest value being the model with the original stellar luminosity. We have not been able to reproduce the very high halo temperatures observed. The maximum (halo–core) T_e differences obtained at any point were about 2000 and 800 K for NGC 6543 and 6826 respectively. However, as shown by Fig. 5, measurements of T_e – made at large offsets from the core of the nebula and averaged over a long slit – would yield much smaller differences than these. These computed values are to be compared with the osberved excesses of 6800^{+985}_{-855} and 2600^{+5655}_{-1800} K for NGC 6543 and 6826, respectively.

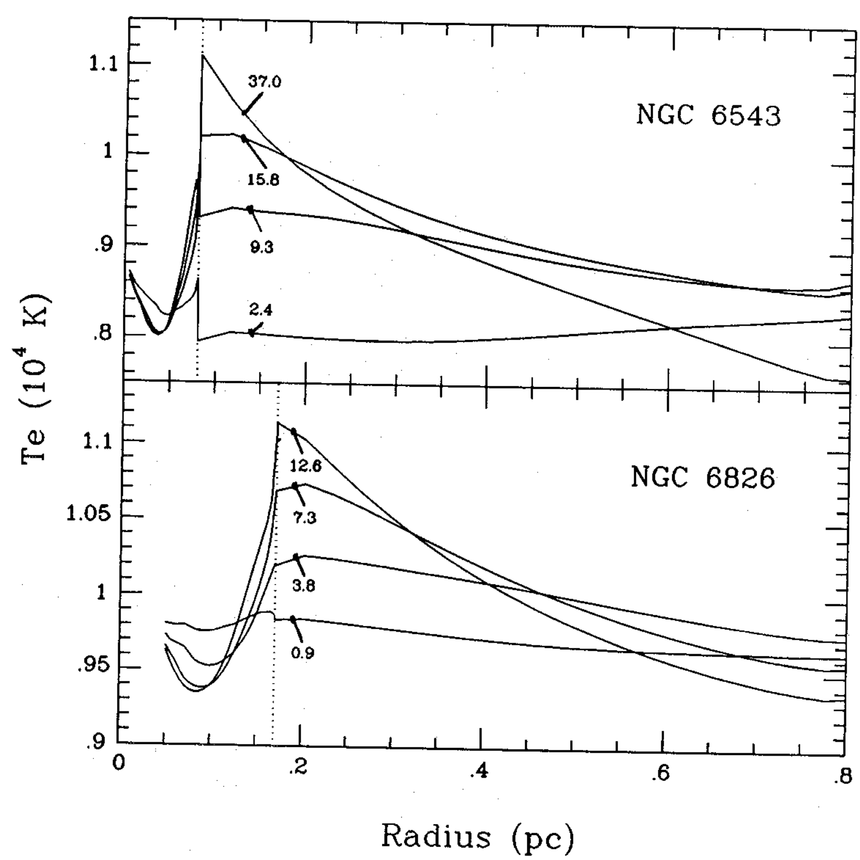

Figure 5. Variation of electron temperature with radius in various photo-ionization models of NGC 6543 and 6826. Each plot is labelled with τ(H I) for the entire model. The dotted line indicates the border between the core and the halo of the planetary nebula.

Some part of the temperature excess observed in these two haloes might be due to the lower abundances measured there (through a reduction in the rate of cooling by collisionally excited lines). We were unable to calculate photo-ionization models with different abundances in different shells, but we have compared pairs of models of the whole NGC 6543 system with either the 'core' or the 'halo' abundances throughout. These models were adjusted slightly so that each member of a pair had the same optical depth in the H I Lyman continuum, so as to avoid changes in the halo cooling rates caused by changing ionic fractions of the heavy elements. We found that for an optically thick pair [τ(H I) = 15.8] an increase in the temperature excess of about 300 K was obtained for a low-abundance halo around a higher-abundance core; for a thin pair of models [τ(H I) = 1.35] the excess increased by about 2000 K (thus giving an excess of 1400 K, as the original excess was -600 K, i.e. the core abundance model had the halo temperature lower than the core temperature).

We conclude that optically thick PN cores do not provide the required temperature excess, and that the combination of thick core plus low-abundance haloes could perhaps provide 40 per cent of the observed excess for NGC 6543. Another method for investigating the temperature is that of energy-balance (see e.g. Preite-Martinez & Pottasch 1983). We find that the halo requires a central star effective temperature (for a blackbody) of 400 000 K while the core only requires one of 37 000 K (*cf.* $T_{\rm Zan} = 43\,000$ K). It seems that some other heating mechanism in the halo must be required. It is possible that the hot fast stellar wind may be leaking into the halo and producing shock excitation. Velocity information is needed to investigate this. We have not examined this further as the shock models available at present (e.g. Shull & McKee 1979) do not include photo-ionization by a hot local star which would alter the excitation of the post-shock gas considerably.

It can be seen from Tables 1 and 2 that [O I]λ6300 emission is on average very much stronger in the haloes than in the cores. Hence we consider whether a significant amount of neutral gas resides in the haloes; this could affect the halo mass and abundances. (The larger the H^0 contribution the smaller the actual abundances become.) We tried to estimate the neutral contribution in NGC 6543 using our photo-ionization models. The model with τ(H I) = 15.8 had 40 per cent H^0 and 22 per cent He^0. (The ratio of these two quantities depends on the shape of the ionizing radiation field.) However, the same model produced a spectrum in an offset slit very different from that observed. The emission lines from neutral atoms such as [O I]λ6300 were almost a factor 10 too large. The observed [O I] emission may well arise from thin transition regions between ionized and neutral gas. Fig. 3 shows that the [O I] (and [O II]) emission does come preferentially from knots in the halo. In these filamentary haloes the surface area of such regions may be much larger than a model with spherical symmetry can mimic. We cannot rule out large amounts of neutrals, as the photo-ionization models do not reproduce the physical conditions of the haloes adequately. There is certainly neutral helium in the haloes; the abundance we measure there is less than the primordial helium abundance (Shields 1986).

4 Discussion

Our results show that the haloes have different temperatures from the cores. Together with the variations in the O^+/O^{2+} ratios across filaments, seen in Figs 3 and 4, this demonstrates that the halo emission is thermal and not reflection by dust. Moreover the ionized masses in the haloes, while not as large as those suggested by Capriotti (1978), are significant for stellar evolutionary calculations. The NGC 6543 halo contains more mass than the core; this result may be true for NGC 6826 also. Consider the total observed system mass of NGC 6543, for an adopted distance of 1.1 kpc and a central star mass of 0.62 $M_\odot$ (Lucy & Perinotto 1987). The total mass is 0.71 $M_\odot$ excluding the halo, or 0.97–1.63 $M_\odot$ including it.

Is there even more mass in these systems? According to the 2-wind model of Kwok (1983), NGC 6543 should have evolved from a 2 $M_\odot$ progenitor. This would suggest that 0.4–1.0 $M_\odot$ of further material could reside in this system – perhaps as low density ionized gas at even larger distances, or as neutral condensations in the halo. Note that there is still some uncertainty in the initial mass–final mass relation for evolution to the white dwarf stage, as described by Weidemann (1987), and thus we cannot state definitely that there is still 'missing mass' for NGC 6543.

Neutral gas might be present in (i) a cold molecular shell, (ii) small condensations or (iii) mixed with the (partially ionized) halo gas. We consider (i) unlikely because the haloes appear to be so filamentary and empty that ionizing photons must surely leak out of the observed structure. Indeed, in NGC 6543 filaments can be seen on Plate 1 which extend out to 240 arcsec from the central star. These are probably density enhancements in a larger shell outside the halo rather than independent bodies, and would then illustrate the point that ionizing photons are escaping from the system. Thus any outer shell is probably ionized, but unobserved because of its low surface brightness.

Possibility (ii) is of interest as some of the observed filaments could be optically thick in H I. This is seen especially at the halo edges (see Figs 3 and 4) where the O^+/O^{2+} ratio can rise markedly. Strong [O I]λ6300 emission in the NGC 6543 halo may also point to optically thick filaments, as noted earlier. It is clear that the inner filaments are genuine density enhancements, as the [O II] emission increases more than the [O III]. (For a gas with most oxygen in the form O^{2+}, the [O III] emission scales as N_e^2 but the [O II] emission as N_e^3.) The sharp change in O^+/O^{2+} seen at the halo edge in Fig. 4 is puzzling – is this a Strömgren radius effect due to an optically thick filament, or a projection effect whereby some distant material shows $N(O^+) > N(O^{2+})$ due to the geometrical dilution of the ionizing radiation? Possibility (iii) was discussed in connection with the photo-ionization models of the haloes in Section 3.4.2, where we concluded that probably not more than 10 per cent of neutral gas is mixed with the ionized gas.

We consider it quite likely that more mass does exist and that it is mainly in the form of an outer shell which is probably ionized.

The limits we have found for the halo mass, together with the fact that the 'edge' of the halo is not a simple Strömgren radius, suggest that the calculations of Capriotti (1978) giving supermassive haloes greatly overestimate the masses.

Our data show that the structures of the haloes are quite inhomogeneous. Fig. 2 illustrates the spatial variation we have found in the halo of NGC 6826, in the emission of [O III]λ5007 at both slit positions. The edge of the halo is quite sharp, suggesting that the mass loss of which the halo is a result increased dramatically from its previous rate. The profile in the slit offset of 46 arcsec is suggestive of the existence of subshells, or knots and filaments, within the halo. Unlike NGC 6543, the [O II]/[O III] ratio is almost constant in this halo – even at the sharp edges. This suggests that the limb brightening is caused by the halo being a thin shell rather than density enhancement in a filled sphere; however, velocity data is required to confirm this. The sharp edge to the halo and the considerable difference in density between the halo and core in both PNe would be consistent with the interacting wind models developed by Kwok, Purton & Fitzgerald (1978) and Volk & Kwok (1985).

A bright knot in the NGC 6826 halo can be seen in Plate 2, and also in the spectrum at position 2 (Fig. 2). We estimate its size to be 7.5 × 9 arcsec, considerably larger than a field star, and it emits strongly in [O III]. We consider it to be a part of the halo; it may have been formed by some interaction with the local interstellar environment.

The abundances measured for the halo appear to be lower than those found for the core. Such composition differences would not agree with current stellar evolution theory (e.g. Iben & Renzini 1983). In particular, the oxygen abundance, which is perhaps the best measured, is not predicted to rise significantly during the last 10^5 yr of stellar evolution on the AGB. (Note that the 'expansion age' of the haloes, $\sim (V_{exp}/10\ \mathrm{km\ s^{-1}}) \times 10^5$ yr, is significantly shorter than a typical lifetime on the AGB (10^6 yr).

The halo abundances calculated from the apparent mean T_e, deduced from the [O III]4363/5007 Å line ratio, could differ from their 'true' values if temperature fluctuations existed within the halo. The theory of allowance for such fluctuations was developed by Peimbert (1967, 1971) and later applications were given by Rubin (1969). We determined the size of the fluctuation parameter t^2 in the halo which would cause the oxygen abundance there to be underestimated by a factor 2.2 (i.e. thus to force equality between the NGC 6543 core and halo O/H ratios). Using T_e([O III]4363/5007) = 14 700 K together with Rubin's equations 8, 10 and 11, we found that a mean temperature $T_0 = 11\ 700$ K and $t^2 = 0.11$ would be required. This is a remarkably large fluctuation parameter.

Observations of the spatial variation in the 4363/5007 Å ratio across the west knot or between slit positions 1 and 2 yield an upper limit to large-scale, resolved fluctuations in T_e. We considered a slab of ionized gas with uniform densities N_e and $N(O^{2+})$ and a temperature law $T_e(z) = T_0 + \Delta T \sin z$. For this case $t^2 = 0.5(\Delta T/T_0)^2$, and the observed mean amplitude of 3750 K corresponds to an 'observed' t^2 of 0.03. The required value of 0.11 would correspond to an amplitude ΔT of 12 600 K! Unless microscopic (unresolved) fluctuations occur, we thus conclude that temperature variations in the halo of NGC 6543 cannot alone explain the apparently low oxygen abundance there.

The low abundances do depend on the measured strength of [O III]λ4363, which provides information on the electron temperature. The measurement of this line seems reliable, and Fig. 1 shows clearly how strong it is relative to the Hγ line. Although the core and halo abundances of NGC 6826 would be very similar if the core temperature were used for both shells, this is not the case for NGC 6543: if the core temperature is adopted for the halo of this system, the halo oxygen abundance would be a factor 4 greater than in the core. (Equal O abundances would be obtained if the electron temperature in the halo was 11 100 K.) This would be in even greater disagreement with current evolutionary theory, and again directly suggests that the halo is hotter than the central nebula.

5 Conclusion

We have shown that the giant haloes of NGC 6543 and 6826 emit thermally. They both have electron temperatures higher than their respective centrally ionized nebulae. The abundances in the haloes appear to be lower, by factors of about 2, than the cores. We have put limits on the halo masses by finding lower and upper limits to the halo electron density. The combined mass of the individual systems is significant for stellar evolutionary theory, and more mass may exist in an even larger shell outside the halo. The fast stellar wind is probably shock heating the halo filaments.

Acknowledgments

We thank D. F. Malin of the AAO for providing the contrast-enhanced image of NGC 6543. Dr E. A. Valentijn provided valuable assistance with the observations, and Drs I. Skillen and R. W. Argyle supplied information on the extinction at La Palma during our observations. DM and RESC were supported by the SERC. JRW aknowledges receipt of a Royal Society European Visiting Fellowship.

References

Aller, L. H. & Czyzak, S. J., 1979. *A. Space Sci.*, **62,** 397.
Aller, L. H. & Czyzak, S. J., 1983. *Astrophys. J. Suppl.*, **51,** 211.
Barker, T., 1983. *Astrophys. J.*, **267,** 630.
Barker, T., 1988. *Astrophys. J.*, **326,** 164.
Bridger, A., 1987. *SERC Starlink User Note No. 86.*
Butler, K. & Mendoza, C., 1984. *Mon. Not. R. astr. Soc.*, **208,** 17P.
Capriotti, E. R., 1978. *IAU Symp. No. 76*, p. 267, ed. Terzian, Y., Reidel, Dordrecht.
Castor, J. I., Lutz, J. H. & Seaton, M. J., 1981. *Mon. Not. R. astr. Soc.*, **194,** 547.
Chu, Y.-H., Jacoby, G. H. & Arendt, R., 1987. *Astrophys. J. Suppl.*, **64,** 529.
Clegg, R. E. S., Peimbert, M. & Torres-Peimbert, S., 1987. *Mon. Not. R. astr. Soc.*, **224,** 761.
Clegg, R. E. S. & Middlemass, D., 1987. *Mon. Not. R. astr. Soc.*, **228,** 759.
Cudworth, K. M., 1974. *Astr. J.*, **79,** 1384.
Giddings, J., 1983. *SERC Starlink User Note No. 37.*
Harrington, J. P., Seaton, M. J., Adams, S. & Lutz, J. H., 1982. *Mon. Not. R. astr. Soc.*, **199,** 157.
Hippelein, H. H., Baessgen, M. & Grewing, M., 1985. *Astr. Astrophys.*, **152,** 213.
Iben, I. & Renzini, A., 1983. *Ann. Rev. Astr. Astrophys.*, **21,** 279.
Jewitt, D. C., Danielson, G. E. & Kupferman, P. N., 1986. *Astrophys. J.*, **302,** 727.
Kaler, J. B., 1976. *Astrophys. J. Suppl.*, **31,** 517.
Kaler, J. B., 1978. *Astrophys. J.*, **226,** 977.
Kaler, J. B., 1983. *Astrophys. J.*, **264,** 594.
King, I. R., 1971. *Publs astr. Soc. Pacif.*, **83,** 199.
Kwok, S., 1983. *IAU Symp. No. 103*, p. 293, ed. Flower, D. R., Reidel, Dordrecht.
Kwok, S., Purton, C. R. & Fitzgerald, P. M., 1978. *Astr. J.*, **219,** L125.
Lucy, L. B. & Perinotto, M., 1987. *Astr. Astrophys.*, **188,** 125.
Mendoza, C., 1983. *IAU Symp. No. 103*, p. 143, ed. Flower, D. R., Reidel, Dordrecht.
Millikan, A. G., 1974. *Astrophys. J.*, **79,** 1259.
Oke, J. B., 1974. *Astrophys. J. Suppl.*, **27,** 21.
Peimbert, M., 1967. *Astrophys. J.*, **150,** 825.
Peimbert, M., 1971. *Bol. Obs. Tonant. y Tacub.*, **6,** 29.
Phillips, J. P. & Reay, N. K., 1983. *Astr. Astrophys.*, **117,** 33.
Phillips, J. P., Reay, N. K. & Worswick, S. P., 1977. *Astr. Astrophys.*, **61,** 695.
Preite-Martinez, A. & Pottasch, S. R., 1983. *Astr. Astrophys.*, **126,** 31.
Rubin, R. H., 1969. *Astrophys. J.*, **155,** 841.
Shields, G., 1986. *Proc. 13th Texas Symp. Rel. Astrophys.*, Chicago, 1986. World Science, Singapore.
Shull, J. M. & McKee, C. F., 1979. *Astrophys. J.*, **227,** 131.
Stone, R. P. S., 1977. *Astrophys. J.*, **218,** 767.
Volk, K. & Kwok, S., 1985. *Astr. Astrophys.*, **153,** 79.
Weidemann, V., 1987. *Astr. Astrophys.*, **188,** 74.
Witt, A. N., Walker, G. A. H., Bohlin, R. C. & Stecher, T. P., 1982. *Astrophys. J.*, **261,** 492.